Journal of Environmental Chemical Engineering 2 (2014) 1748–1755

Contents lists available at ScienceDirect

Journal of Environmental Chemical Engineering

journal homepage: www.elsevier.com/locate/jece

Chemically grown TiO_2 on glass with superior photocatalytic properties

G. Kenanakis [a,b,*], N. Katsarakis [a,b]

[a] Institute of Electronic Structure and Laser, Foundation for Research & Technology – Hellas, P.O. Box 1385, Vassilika Vouton, Heraklion, Crete 711 10, Greece
[b] Center of Materials Technology and Photonics, School of Applied Technology, Technological Educational Institute of Crete, Heraklion, Crete 710 04, Greece

ARTICLE INFO

Article history:
Received 12 May 2014
Accepted 14 July 2014

Keywords:
Titanium dioxide thin films
Degussa P25 TiO_2
Sol–gel technique
Photocatalysis
Stearic acid
Methylene blue

ABSTRACT

TiO_2 anatase and Degussa (Enovik) P25 thin films were deposited on glass using the sol–gel technique at 600 and 80 °C, respectively. The structural, morphological and optical properties of the as-grown TiO_2 films were studied against their thickness, for both of the experimental procedures described. Moreover, the photocatalytic activity of the TiO_2 samples was investigated regarding the degradation of stearic acid and the decolorization of methylene blue, under UV-A light illumination. In specific, the 90 nm-thick (4×) Degussa P25 TiO_2 films deposited on glass at 80 °C is by far the more photocatalytically active against methylene blue decolorization, reaching an apparent rate constant of 0.094 min^{-1}, while the photocatalytic activity of the 110 nm-thick (4×) TiO_2 thin films deposited on glass at 600 °C by sol–gel show the highest stearic acid disappearance rate, i.e., 9.46×10^{-8} mol/min (formal quantum efficiency = 10.02×10^{-3}) at 15 min of UV-A light illumination.

Introduction

Development of immobilized TiO_2 films has attracted large scientific interest due to their interesting electrochemical and photocatalytic properties that are widely applied in the field of photocatalysis for various applications such as water treatment, air purification and fuel cells [1–5].

TiO_2 nanopowders, even though they exhibit a high photocatalytic efficiency, they have mostly been used in water suspensions or in small-scale purification systems, thus limiting their practical use due to difficulties in their separation and recovery [1–4]. Supporting photocatalytic materials on a steady substrate can eliminate this issue, opening a whole new range of applications, targeting the decomposition of organic substances originally adsorbed on the surfaces [6,7]. Based on such understanding, many photocatalytic semiconductors including TiO_2 have been already prepared as thin films as well as fine powders using several deposition techniques [8–10]. Since then, many large scale deposition techniques, such as doctor blade and spray coating, have been adopted in order to produce TiO_2 coated surfaces with photocatalytic and self-cleaning properties [1,7,11–13].

It is generally known that anatase structure of TiO_2 is more efficient as a photocatalyst than rutile, because of its higher energetic level, which enables a higher reduction potential [14]. However, the existence of the anatase phase is not the only essential condition for high efficiency; the photocatalytic activity of TiO_2 thin films can vary considerably and is dependent on many factors, such as film thickness, roughness, grain size and deposition temperature, to name but a few. Hence, it is important to develop deposition methods by which these properties can be controlled.

A common deposition procedure for TiO_2 coatings on steady substrates is the sol–gel technique using alkoxide precursors [15], which determines the grain size, structure, phase and density of sol–gel derived films [16,17].

In this work, we study the photocatalytic properties of TiO_2 thin films, deposited via sol–gel on glass substrates at 600 °C, using alcoholic solutions. The photocatalytic properties of the as-deposited TiO_2 thin films regarding the degradation of stearic acid and the decolorization of methylene blue in aqueous solution under UV-A light illumination are investigated. In particular, the effect of film thickness and grain size of the TiO_2 thin films on their photocatalytic activity is comprehensively studied. Finally, in order to have a straight comparison in the photocatalytic activity between the sol–gel deposited TiO_2 thin films and a reference material, Degussa (Enovik) P25, Aeroxide TiO_2 P25 films, were also

* Corresponding author at: Institute of Electronic Structure and Laser (IESL), Foundation for Research & Technology – Hellas (FORTH), P.O. Box 1385, Vasilika Vouton, 71110 Heraklion, Crete, Greece. Tel.: +30 2810 391917; fax: +30 2810 391951.
E-mail address: gkenanak@iesl.forth.gr (G. Kenanakis).

http://dx.doi.org/10.1016/j.jece.2014.07.015
2213-3437/

prepared via spin-coating and photocatalytically characterized under the same conditions.

Experimental details

Synthesis of TiO_2 films

TiO_2 thin films using the sol–gel technique

The procedure for preparing the TiO_2 films immobilized on glass ($10 \times 10\,mm^2$ Corning Eagle 2000 Borosilicate Glass, Specialty Glass Products) is similar to that reported in [18–20]. The reagents, include commercial ultrapure titanium isopropoxide (99.999%, Sigma–Aldrich), absolute ethanol (99.8%, Sigma–Aldrich), and acetyleacetone (99.5%, Fluka). 2.8 ml of titanium isopropoxide, was first dissolved in 25 ml of absolute ethanol. The resultant solution was stirred for 15 min at room temperature using a magnetic stirrer to yield a homogeneous, clear and transparent solution. 0.1 ml of acetylacetone was added to the solution as a stabilizing agent, reacting with the alkoxide precursor and modifying the ligand structure, as proposed by Sanchez et al. [15]. In such way, the precursor solution becomes less sensitive to humidity (avoiding precipitation), enabling the hydrolysis and polycondensation reactions to be controlled [20,21]. The deposition was usually performed within 24 h after the solution was prepared, by dropping 30 μl of the precursor solution onto glass substrates which were then rotated at 3000 rpm for 30 s. After processing, the substrates were pre-heated at 350 °C for 10 min to evaporate the solvent and remove the organic residuals from the films. This procedure was repeated up to 4 times (1×, 2×, 3×, 4× times). The films were then annealed in air at 600 °C for 120 min.

Degussa (Enovik) P25 TiO_2 films

1×, 2× and 4× films of Degussa (Enovik) P25, Aeroxide TiO_2 P25, were also prepared and used in order to have a comparison in photocatalytic activity between the as-grown TiO_2 thin films and a reference material. Thus, Degussa P25 TiO_2 films on glass substrates were cast by spin-coating on glass ($10 \times 10\,mm^2$ Corning Eagle 2000, Borosilicate Glass, Specialty Glass Products) with a 5% (w/v) aqueous slurry of Degussa P25 TiO_2 [22–24]. 30 μl of the Degussa P25 slurry was deposited on the center of the glass substrates and then spun at 3000 rpm for 30 s. The films were then washed with ultrapure water (18.2 MΩ cm) and dried, first in an N_2 gas flow and then in an oven at 80 °C for 1 h.

Prior to deposition, all glass substrates used were cleaned using a Piranha solution ($H_2SO_4/H_2O_2 = 3/1$), rinsed with ultrapure water and dried under N_2 gas flow. Finally, the thickness of the all TiO_2 films was measured using a stylus profilometer (alpha-step 100, Tencor).

Characterization techniques

The crystal structure of all samples was determined by X-ray diffraction (XRD) using a Rigaku (RINT 2000) diffractometer with Cu *Ka* X-rays, while Raman measurements were carried out using a model Raman spectrometer (Jobin Yvon, ISA – Horiba group model T-64000), with a 514.5 nm line of an air-cooled Ar^+ laser (Spectra-Physics 163-A42) and wavenumber range 50–750 cm^{-1}. The surface morphology of the TiO_2 thin films was studied by means of a field emission scanning electron microscope (FE-SEM, JEOL JSM-7000F) and an atomic force microscope (AFM) in tapping mode (Digital Instruments – Nanoscope IIIa), while the surface roughness (RMS) of the as-deposited samples was determined using the scanning probe image processor (SPIP, v. 3.3.5.0) image processing software for nano- and micro-scale microscopy from Image Metrology. Finally, UV–vis transmission spectra were recorded using a Shimadzu UV-2401 spectrophotometer over the wavelength range of 250–950 nm.

Photocatalytic activity studies

There are many different methods that can be used to determine the activity of photocatalytic surfaces. Popular techniques include those based on the photo-oxidation of organic films such as stearic acid [9,23–28], the decolorization of methylene blue in aqueous solutions [29–32], or contact angle changes [24].

Stearic acid test

The photocatalytic activity of the as-grown TiO_2 thin films was firstly determined using stearic acid (SA) as a model compound, in which a thin layer of SA is deposited onto the examined sample and its photocatalytic destruction is monitored as a function of time [9,23–28]. This method has gained preference over the years since SA provides a reasonable model compound for solid films that deposit on exterior and interior surfaces. Moreover, SA is very stable under UV illumination in the absence of a photocatalyst film (phenomenon of photolysis). Furthermore, SA can be easily laid down from a methanol or chloroform solution making the test much easier.

A 0.1 M SA (98.5%, Sigma–Aldrich) solution in chloroform was spin-coated on the sample surface under test at a rotation speed of 500 rpm for 30 s. Samples were then dried at 80 °C in air for 10 min.

The decomposition of SA can be demonstrated by FT-IR spectroscopy through the monitoring of the asymmetric C—H stretching mode of the CH_3 group at 2958 cm^{-1} and the asymmetric and symmetric C—H stretching modes of the CH_2 group at 2923 and 2853 cm^{-1}, respectively. The photocatalytic activity experiments for all TiO_2 samples regarding the decomposition of SA were performed in ambient air and were repeated for five times demonstrating no changes in the % SA conversion, i.e., the observed photocatalytic activity variations were in the order of ∼2–3%. The integrated area of the SA C—H stretching peaks (2800–3000 cm^{-1}) was monitored using a Fourier transform infrared spectrometer (FT-IR, IRPrestige-21, Shimadzu) before and after black light illumination in a box reactor at certain time intervals. The light source used was an HPK 125 W Philips mercury lamp with main emission wavelength at 365 nm and an incident light intensity of ∼8.9 mW/cm^2. For ease in comparison of the photocatalytic activity between different samples, the integrated area of the C—H stretching peaks (2800–3000 cm^{-1}) measured at each irradiation time interval was normalized to the initial integrated area (prior to the irradiation) in order to calculate the percentage of SA remaining as a function of irradiation time. Blank experiments (photolysis) were also performed using bare glass substrates under exactly the same conditions applied for the TiO_2 samples. Finally, the SA disappearance rate (mol/min) and the formal quantum efficiency (FQE) for all TiO_2 thin films were calculated according to the methodology of by Mills and Wang [23] and Paz et al. [33].

Methylene blue test

The photocatalytic activity of the TiO_2 samples was also quantified by means of the decolorization of methylene blue (MB) in aqueous solution, which is a typical potent cationic dye that has been widely used as a model organic to probe the photocatalytic performance of photocatalysts [29–32]. 1 ml of MB (82%, Sigma–Aldrich) solution at an initial concentration of 5.4×10^{-7} mol/l (20 ppm) and a pH value of 5.5, was put in a quartz cell with a surface of ∼100 mm^2. A sample of rectangular geometry (area of $10 \times 10\,mm^2$) was immersed into the cell and this arrangement (cell + solution + sample) was placed inside a homemade reactor equipped with aluminum reflector sides. Five

UV-A type lamps (vertically overhead of the samples) which predominantly emit at 365 nm (4 W, Philips TL 4 W/08) were used as UV source. The distance between cell and lamps was 13 cm, while the light intensity inside the reactor was ~1.6 mW/cm^2. The MB concentration (decolorization) was monitored by UV–Vis spectroscopy (absorption at λ_{max}, 665 nm) [29–32] using a Shimadzu UV-2401 spectrophotometer.

As in the case of SA test, photolysis experiments were also performed using bare glass substrates under exactly the same conditions applied for the TiO_2 samples.

Results and discussion

Fig. 1 depicts typical X-ray diffraction patterns of the TiO_2 thin films deposited by the sol–gel/spin-coating technique after 1, 2, 3 and 4 spinning cycles at 600 °C. The thickness of the 1×, 2×, 3× and 4× TiO_2 thin films is ~30, ~50, ~70 and ~110 nm respectively. The diffraction peaks observed for the TiO_2 thin films 25.34°, 37.84°, 48.18° and 54.02° (see Fig. 1(a–c)) are in good agreement with the JCPDS card (No. 84-1286) for the crystal structure of anatase [21–26]. It can be also seen that no other characteristic peaks corresponding to possible impurities are observed in the XRD patterns. Moreover, it can be observed from Fig. 1(a–c) that 4× TiO_2 thin films show narrower XRD reflections with significantly higher intensity than the corresponding 1×, 2× and 3× TiO_2 samples, indicating in general an enhanced crystallinity of the TiO_2 thin films with increasing thickness.

Fig. 2 shows a typical Raman Spectrum of the as-grown TiO_2 thin films grown on glass at 600 °C. It is of great significance that all samples (1×, 2×, 3× and 4×) exhibit characteristic TiO_2 phonon structure in the Raman Spectra obtained. The observed phonon frequencies, matching (±2 cm^{-1}) with literature [28,34] for anatase TiO_2 are: 145 cm^{-1} (E_g), 200 cm^{-1} (E_g), 399 cm^{-1} (B_{1g}), 519 cm^{-1} (A_{1g}) and 642 cm^{-1} (E_g).

Fig. 3(a–d) presents AFM images (scan size 1 × 1 μm) of the 30 nm – (1×), 50 nm – (2×), 70 nm – (3×) and 110 nm-thick (4×) TiO_2 thin films deposited on glass substrates via sol–gel at 600 °C, respectively. It can be observed that all the TiO_2 thin films are homogeneous, crack-free and densely packed, while their grains are significant small. Fig. 3(e) exhibits the variation of grain size (black squares) and surface roughness (RMS, blue stars) of the as-grown TiO_2 thin films as a function of the number of spin-coated layers.

From Fig. 3 one can notice that the as-grown TiO_2 thin films have low roughness (1.3–1.8 nm) and a relatively small variation in grain size (15.8 ± 2–19 ± 3 nm) for a number of spinning cycles (1×–4×, 30–110 nm thick samples), indicating the stability of the as-grown samples using the sol–gel technique in a wide range of thicknesses.

The optical transmittance spectra of the 1×–4× TiO_2 thin films grown at 600 °C in the wavelength region 250–950 nm are presented in Fig. 4. All the TiO_2 thin films are highly transparent in the visible wavelength region with an average transmittance of about 80–90%, with a fall-off for wavelengths shorter than 350 nm. Furthermore, the optical energy gap values (E_{gap}) of the TiO_2 thin films were determined by the extrapolation of the linear portion of $(\alpha h\nu)^2$ vs. $h\nu$ plots ("*Tauc*" plots). The values obtained for the TiO_2 thin films vary from 3.61 (1× TiO_2) to 3.45 eV (4× TiO_2), similar to the ones reported by [35,36] for anatase TiO_2 thin films obtained using sol–gel approaches. As seen, the estimated values of the band gap for the as-grown TiO_2 thin films are larger than for bulk TiO_2 (3.3 eV), since the films consisting of fine crystallites show "blue shift" [37]. Moreover, one can see that energy band gap of the TiO_2 thin films decrease with thickness (number of spinning layers). This decrease was correlated with grain size increase (as seen in Fig. 3), since when the latter increases the defects and impurities tend to disappear causing a reorganization of the structure.

The decrease of MB concentration (decolorization) for the 1×–4× TiO_2 thin films under UV-A light irradiation is presented in Fig. 5(a). For comparison reasons, the photolysis curve (no catalyst present) is also displayed. According to the photolysis (black) curve in Fig. 5(a), the MB concentration remained almost constant (decreasing from 100 to ~96%) during ~120 min irradiation, indicating that the photolysis of MB was almost negligible. All the TiO_2 thin films displayed significant photocatalytic activity, as recorded by the dramatic decrease of the MB concentration, due to the highly oxidative radicals generated on the TiO_2 surfaces under UV-A irradiation [38]. Moreover, the 110 nm-thick (4×) TiO_2 thin film showed better photocatalytic activity, giving ~93% MB concentration reduction after 60 min irradiation (and ~97% MB concentration reduction after 90 min). Table 1 summarizes the photocatalytic activity of the TiO_2 thin films regarding the decolorization of MB at 60 and 90 min exposure under UV-A illumination. In addition, the apparent rate constant (k) has been

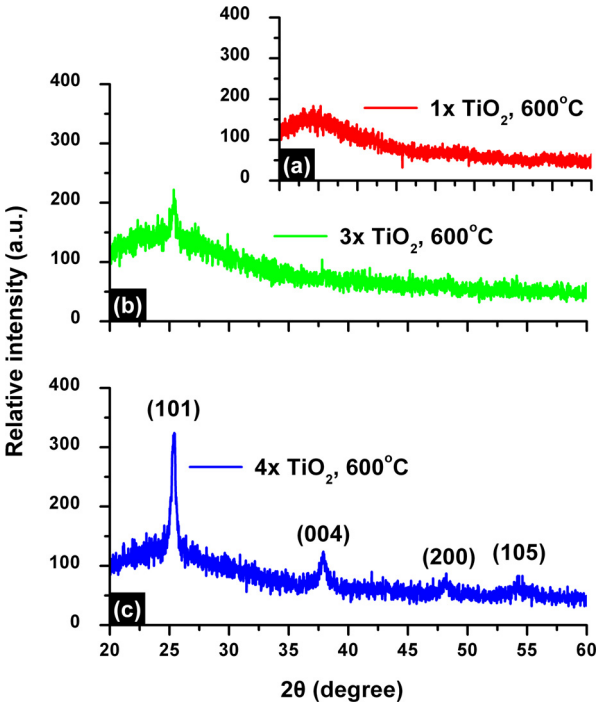

Fig. 1. X-ray diffraction patterns of the TiO_2 thin films deposited by the sol–gel/spin-coating technique after 1 (a), 3 (b) and 4 (c) spinning cycles at 600 °C.

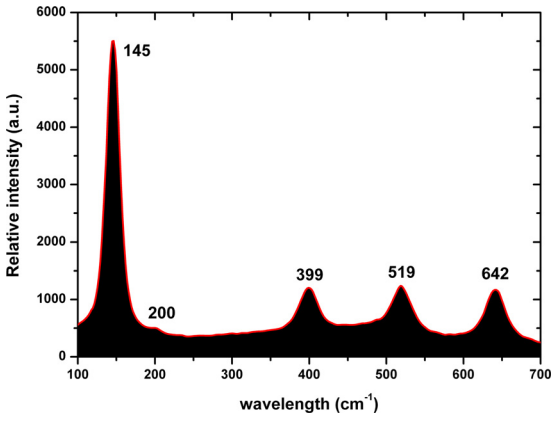

Fig. 2. Typical Raman spectrum of the as-grown TiO_2 thin films deposited on glass by the sol–gel/spin-coating technique at 600 °C.

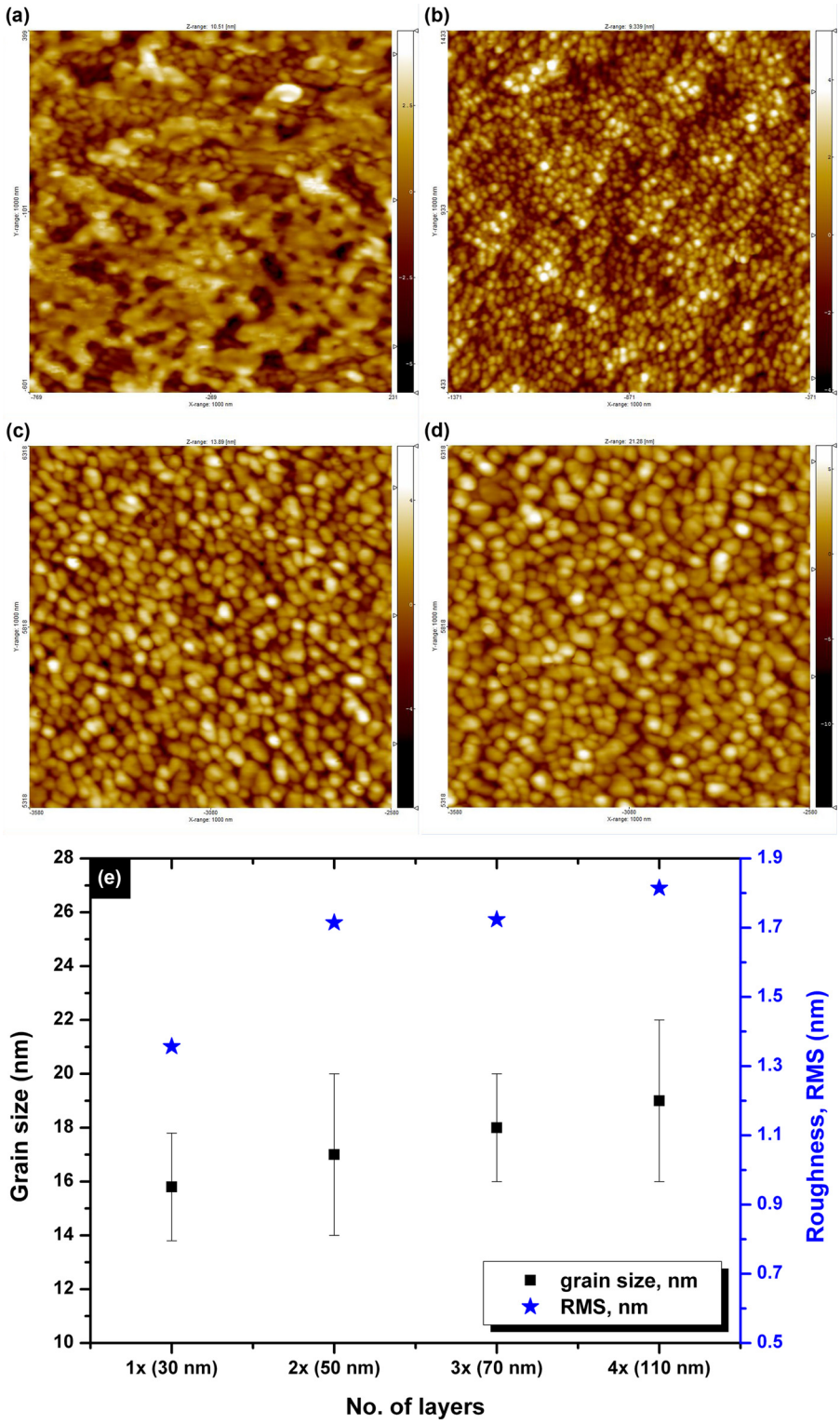

Fig. 3. AFM images (scan size 1 μm × 1 μm) of the 1× (a), 2× (b), 3× (c), and 4× (d) TiO_2 thin films deposited on Corning glass substrates via sol–gel at 600 °C, respectively. The grain size (black squares) and surface roughness (RMS, blue stars) of the as-grown TiO_2 thin films as a function of number of spin-coated layers is presented in (e).

calculated as the basic kinetic parameter for the comparison of photocatalytic activities, which was fitted by the equation $\ln(C_t/C_0) = -kt$, where k is apparent rate constant, C_t is the concentration of MB, and C_0 is the initial concentration of MB. It should be noted that the adjusted R-square statistic varies from 0.99823 to 0.99915 indicating that the model used for the determination of the apparent rate constant (k) is adequate. The good linear fit of equation $\ln(C_t/C_0) = -kt$, shown in the inset of Fig. 5(a), confirms that the photodegradation of MB over TiO_2 photocatalysts follows first-order kinetics. The calculated apparent rate constants were 0.020, 0.029, 0.042 and 0.054 min^{-1} for the 1×, 2×, 3× and 4× TiO_2 thin films, respectively.

Fig. 5(b) presents the normalized integrated area of SA vs. irradiation time curves for 1×–4× TiO_2 thin films deposited by

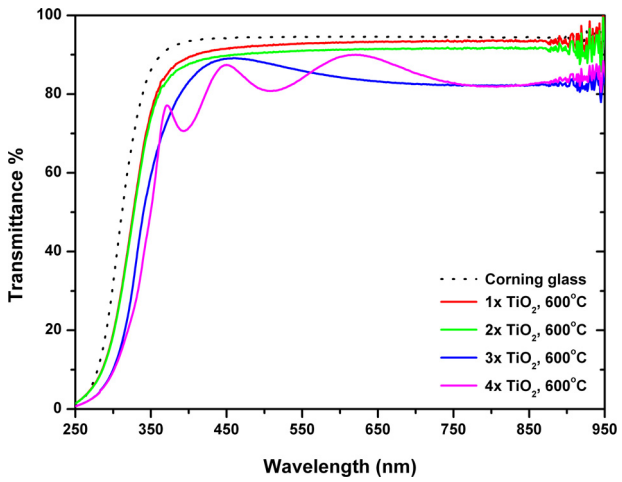

Fig. 4. Optical transmittance spectra of the 1×–4× TiO_2 thin films grown at 600 °C in the wavelength region 250–950 nm.

sol–gel on Corning glass at 600 °C. For comparison reasons, the photolysis curve (no catalyst present) is also displayed. Table 2 summarizes the photocatalytic activity of the TiO_2 thin films regarding the degradation of SA at 15 min exposure of UV-A illumination. Following the methodology explained by Mills and Wang [23] and Paz et al. [33], the SA disappearance rate (mol/min) and the formal quantum efficiency (FQE) at 15 min exposure under UV-A illumination were calculated for all the TiO_2 thin films deposited at 600 °C. As one can notice from Table 2, the photocatalytic activity of all the TiO_2 thin films regarding the % decomposition of SA (as well as the FQE and SA disappearance rates) is always significantly higher than that observed due to photolysis, i.e., light irradiation of SA in the absence of a TiO_2 catalyst. Furthermore, if one takes into account the XRD data from Fig. 1, he will notice that the photocatalytic activity of the TiO_2 thin films is closely associated to their crystallinity. Thus, the 4× TiO_2 thin film shows a FQE value of $\sim 10.02 \times 10^{-3}$ and a SA disappearance rate of $\sim 9.46 \times 10^{-8}$ mol/min at 15 min, while the corresponding values of FQE and SA disappearance rate for 3×, 2× and 1× TiO_2 thin films deposited at 600 °C are $\sim 8.05 \times 10^{-3}$/$\sim 7.60 \times 10^{-8}$ mol/min, $\sim 5.24 \times 10^{-3}$/$\sim 4.95 \times 10^{-8}$ mol/min and 4.03×10^{-3}/$\sim 3.81 \times 10^{-8}$ mol/min, respectively. Moreover, it should be noted that, the 110 nm-thick (4×) TiO_2 thin films deposited at 600 °C show a remarkable photocatalytic activity (FQE = 0.02×10^{-3}), higher to the one reported by Paz et al. [33] following a similar experimental procedure.

Since Degussa (Enovik) P25 TiO_2 powder, is widely used in many photocatalytic reaction systems due to its relatively high levels of photocatalytic activity, we prepared 1×, 2× and 4× Degussa P25 films on glass, according to the methodology of Mills et al. [22–24] in order to compare the as-grown TiO_2 thin films with a standard reference material. The thickness of the 1×, 2× and 4× Degussa P25 TiO_2 films is ∼25, ∼40 and ∼90 nm, respectively.

Fig. 6(a,b) illustrate the XRD pattern and a scanning electron microscope (SEM) picture of the 90 nm-thick (4×) Degussa P25 TiO_2 film. As expected, the diffraction peaks observed for 4× Degussa P25 TiO_2 film correspond to both anatase (marked with "A" in Fig. 6(a)) and rutile phase (marked with "R" in Fig. 6(a)), in good agreement with the JCPDS card (No. 84-1286) and JCPDS card (No. 88-1175) for a crystal structure of anatase and rutile, respectively [39,40].

From Fig. 6(b) one can see that the 90 nm-thick (4×) Degussa P25 TiO_2 film consists of TiO_2 nano-spheres with a diameter varying from 16–30 nm, in agreement with the nominal mean diameter of the Degussa P25 samples which is ∼25 nm. Furthermore, several agglomerations can be observed reaching a diameter of almost 100 nm.

Finally, Fig. 6(c) presents the optical transmittance spectra of the 1×, 2×, and 4× Degussa P25 TiO_2 films, in the wavelength region 250–950 nm, showing that all Degussa P25 samples are highly transparent in the visible wavelength region with an average transmittance of about 90%.

Fig. 7(a,b) presents the decrease of MB concentration (decolorization) and the normalized integrated area of SA vs. irradiation time, for 1×, 2×, and 4× Degussa P25 films under UV-A, using the same experimental condition with the sol–gel TiO_2 films described above. Once more, the inset of Fig. 7(a), confirms that the photodegradation of MB over Degussa P25 TiO_2 films follows first-order kinetics. The calculated apparent rate constants were 0.039, 0.055 and 0.094 min^{-1} for the 1×, 2× and 4× Degussa P25 TiO_2 films, respectively. One can notice that the Degussa P25 TiO_2 films are by far more photocatalytically active that the as-grown TiO_2

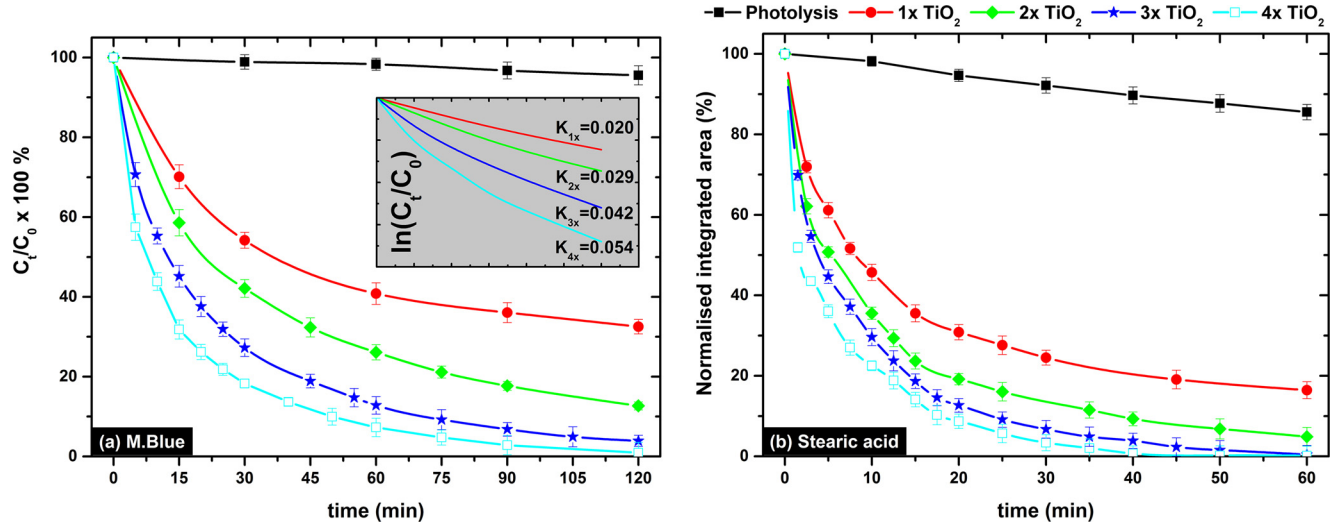

Fig. 5. % MB decolorization over the TiO_2 thin films under UV-A irradiation (a), and the apparent rate constants (k) [inset of (a)]. The normalized integrated area of SA vs. irradiation time curves for 1×–4× TiO_2 thin films deposited by sol–gel on Corning glass at 600 °C is presented in (b). For comparison reasons, the photolysis curve (black solid squares) is also presented.

Table 1
Photocatalytic activity of TiO_2 thin films deposited on glass substrates at 600 °C, regarding the decolorization of MB, at 60 and 90 min of exposure under UV-A illumination.

α (%)	Photolysis (%)	1× TiO_2 (%)	2× TiO_2 (%)	3× TiO_2 (%)	4× TiO_2 (%)
60 min UV-A	1.70	59.18	73.90	87.20	92.73
90 min UV-A	3.25	63.95	82.32	93.19	97.17

Table 2
Photocatalytic activity at 15 min, initial stearic acid disappearance rate (mol/min) and formal quantum efficiency (FQE, see Mills and Wang [23]), for the TiO_2 thin films deposited on glass substrates using the sol–gel technique at 600 °C.

	Photolysis	1× TiO_2	2× TiO_2	3× TiO_2	4× TiO_2
α (%) at 15 min	3.56%	64.45%	76.30%	81.32%	85.89%
Initial SA disappearance rate (mol/min)	3.05×10^{-10}	3.81×10^{-8}	4.95×10^{-8}	7.60×10^{-8}	9.46×10^{-8}
Formal quantum efficiency, $(FQE)_{(SA)}/10^{-3}$	0.03	4.03	5.24	8.05	10.02

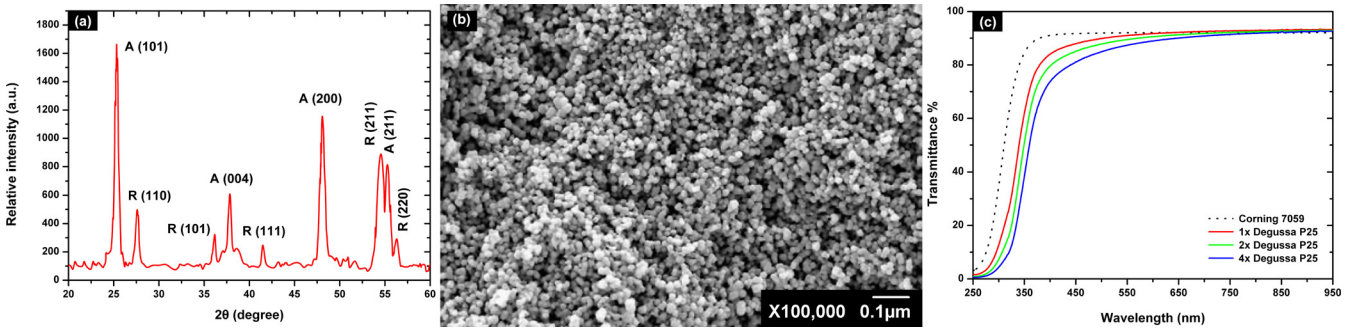

Fig. 6. XRD pattern (a) and SEM picture (b) of our 90 nm-thick (4×) Degussa P25 TiO_2 film. The optical transmittance spectra of the 1×, 2×, and 4× P25 TiO_2 films, in the wavelength region 250–950 nm, are also presented in (c).

thin films at 600 °C, regarding the decolorization of MB, reaching an almost 95% MB concentration reduction after 30 min of irradiation (see the case of 4× P25 films in Fig. 7(a)).

On the other hand, Degussa P25 TiO_2 films are less effective for SA conversion than the TiO_2 thin films deposited using the sol–gel technique at 600 °C. Indeed, we have calculated the FQE and SA disappearance rates for the 1×, 2×, and 4× Degussa P25 TiO_2 films, being $\sim 5.32 \times 10^{-3}/\sim 5.64 \times 10^{-8}$ mol/min, $\sim 4.09 \times 10^{-3}/\sim 4.33 \times 10^{-8}$ mol/min, and $3.15 \times 10^{-3}/\sim 3.34 \times 10^{-8}$ mol/min, respectively, close to the values reported from Mills et al. in [23]. The higher photocatalytic activity of the as-grown TiO_2 thin films can be explained in terms of their large surface area. Since Degussa P25

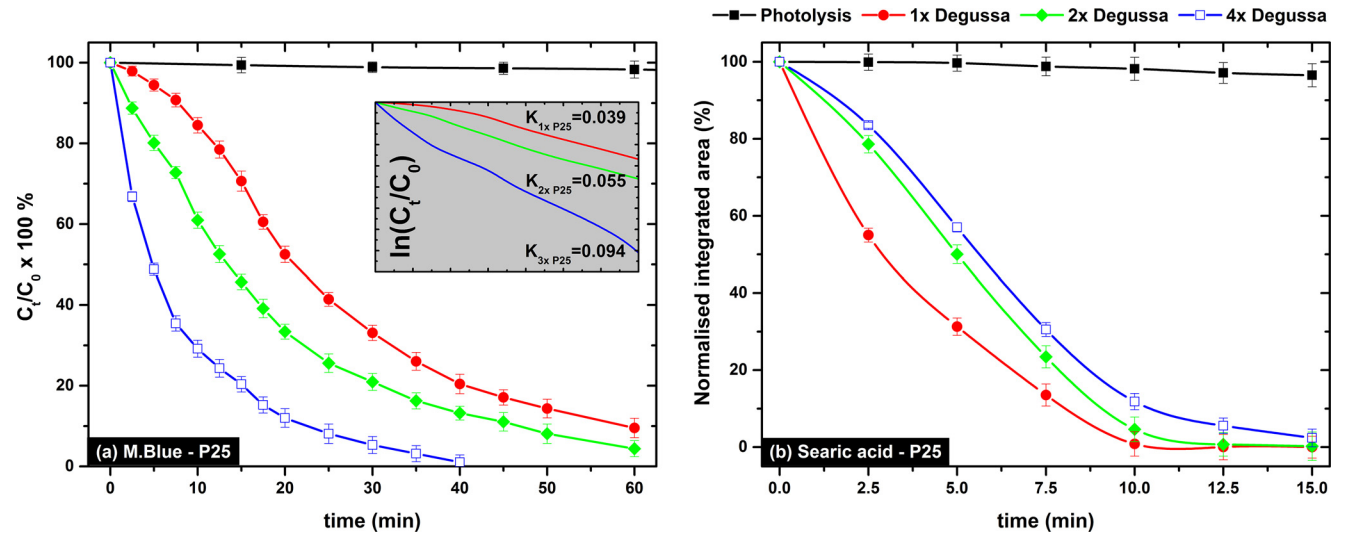

Fig. 7. % MB decolorization (a) and normalized integrated area of SA (b) vs. irradiation time, for 1×, 2×, and 4× P25 films under UV-A irradiation. In the inset of (a) the apparent rate constants of % MB decolorization for the Degussa P25 films are presented.

TiO_2 films were formed by the aggregation of TiO_2 nano-spheres giving agglomerations with a diameter of ~100 nm (see Fig. 6(b)), quite bigger that the grain size of the TiO_2 films derived by the sol–gel technique at 600 °C (15.8 ± 2–19 ± 3 nm) (see Fig. 3), a smaller surface area available for light absorption is obtained for the case of Degussa P25 films, and hence a drop in the photocatalytic degradation rate of SA would be expected.

This surface area effect is not so intense for the case of the decolorization of methylene blue, since the MB aqueous solution "penetrates" easier through the Degussa P25 TiO_2 nano-spheres reaching each one of them, and thus MB is effectively decolorized upon UV-A irradiation, taking advantage of all the surface area available. On the other hand, solid organic compounds that deposit indoors or outdoors, such as SA, are only in touch with the outer area/surface of the catalyst, and thus their degradation is restricted to the outer area/surface only.

Conclusions

Immobilized TiO_2 and Degussa (Enovik) P25 catalysts were deposited on glass using the sol–gel technique at 600 and 80 °C, respectively. The only detectable crystal structure in the TiO_2 thin films deposited on glass by sol–gel at 600 °C is that of anatase, while their grain size varies from 15.8 ± 2 nm–19 ± 3 nm. On the other hand, Degussa P25 films exhibit all the diffraction peaks that correspond to both anatase and rutile phases, while they consist of several agglomerations reaching a diameter of almost 100 nm. Finally, all the TiO_2 samples are highly transparent in the visible wavelength region and show remarkable photocatalytic activity regarding the decolorization of methylene blue and % degradation of stearic acid. In particular, the 110 nm-thick TiO_2 thin film deposited by sol–gel at 600 °C shows a very significant FQE value (10.02×10^{-3}), much higher than that observed for the best Degussa (Enovik) P25 immobilized catalyst (5.32×10^{-3}).

Acknowledgements

This project is implemented through the Operational Program "Education and Lifelong Learning", Action Archimedes III and is co-financed by the European Union (European Social Fund) and Greek national funds (National Strategic Reference Framework 2007–2013).

References

[1] A. Fujishima, X. Zhang, D.A. Tryk, TiO_2 photocatalysis and related surface phenomena, Surf. Sci. Rep. 63 (2008) 515–582, doi:http://dx.doi.org/10.1016/j.surfrep.2008.10.001.
[2] K. Hashimoto, H. Irie, A. Fujishima, TiO_2 photocatalysis: a historical overview and future prospects, Jpn. J. Appl. Phy. 44 (2005) 8269–8285, doi:http://dx.doi.org/10.1143/JJAP.44.8269.
[3] M. Pelaez, N.T. Nolan, S.C. Pillai, M.K. Seery, P. Falaras, A.G. Kontos, P.S.M. Dunlop, J.W.J. Hamilton, J.A. Byrne, K. O'Shea, M.H. Entezari, D.D. Dionysiou, A review on the visible light active titanium dioxide photocatalysts for environmental applications, Appl. Catal. B: Environ. 125 (2012) 331–349, doi:http://dx.doi.org/10.1016/j.apcatb.2012.05.036.
[4] M. Lu, P. Pichat, Photocatalysis and Water Purification: From Fundamentals to Applications, Wiley-VCH, Weinheim, 2013.
[5] Y. Chen, D.D. Dionysiou, Correlation of structural properties and film thickness to photocatalytic activity of thick TiO_2 films coated on stainless steel, Appl. Catal. B: Environ. 69 (2006) 24–33, doi:http://dx.doi.org/10.1016/j.apcatb.2006.05.002.
[6] M.A. Henderson, A surface science perspective on TiO_2 photocatalysis, Surf. Sci. Rep. 66 (2011) 185–297, doi:http://dx.doi.org/10.1016/j.surfrep.2011.01.001.
[7] L. Lopez, W.A. Daoud, D. Dutta, Preparation of large scale photocatalytic TiO_2 films by the sol–gel process, Surf. Coat. Technol. 2 (15) (2010) 251–257.
[8] A. Mills, S. Le Hunte, An overview of semiconductor photocatalysis, J. Photochem. Photobiol. A: Chem. 108 (1997) 1–35, doi:http://dx.doi.org/10.1016/S1010-6030(97)00118-4.
[9] M. Suzuki, T. Ito, Y. Taga, Photocatalysis of sculptured thin films of TiO_2, Appl. Phy. Lett. 78 (2001) 3968–3970, doi:http://dx.doi.org/10.1063/1.1380730.
[10] P.V. Kamat, R. Huehn, R. Nicolaescu, A "sense and shoot" approach for photocatalytic degradation of organic contaminants in water, J. Phy. Chem. B 106 (2002) 788–794, doi:http://dx.doi.org/10.1021/jp013602t.
[11] G.J. Yang, C.J. Li, F. Han, A. Ohmori, Microstructure and photocatalytic performance of high velocity oxy-fuel sprayed TiO_2 coatings, Thin Solid Films 466 (2004) 81–85, doi:http://dx.doi.org/10.1016/j.tsf.2004.02.015.
[12] R. Wang, K. Hashimoto, A. Fujishima, M. Chikuni, E. Kojima, A. Kitamura, M. Shimohigoshi, T. Watanabe, Photogeneration of highly amphiphilic TiO_2 surfaces, Adv. Mater. 10 (2) (1998) 135–138.
[13] A. Fujishima, X. Zhang, Titanium dioxide photocatalysis: present situation and future approaches, Comptes Rendus Chimie 9 (2006) 750–760, doi:http://dx.doi.org/10.1016/j.crci.2005.02.055.
[14] A. Fujishima, K. Hashimoto, T. Watanabe, TiO_2 Photocatalysis – Fundamentals and Applications, BKC, Tokyo, 1999.
[15] C. Sanchez, J. Livage, M. Henry, F. Babonneau, Chemical modification of alkoxide precursors, J. Non-Cryst. Solids 100 (1988) 65–76, doi:http://dx.doi.org/10.1016/0022-3093(88)90007-5.
[16] M. Rahman, G. Yu, T.S. Soga, T. Jimbo, H. Ebisu, M. Umeno, Refractive index and degree of inhomogeneity of nanocrystalline TiO_2 thin films: effects of substrate and annealing temperature, J. Appl. Phy. 88 (2000) 4634–4641, doi:http://dx.doi.org/10.1063/1.1290456.
[17] J. Yuan, S. Tsujikawa, Characterization of sol–gel-derived TiO_2 coatings and their photoeffects on copper substrates, J. Electrochem. Soc. 142 (1995) 3444–3450.
[18] A. Rampaul, I.P. Parkin, S.A. O'Neill, J. DeSouza, A. Mills, N. Elliott, Titania and tungsten doped titania thin films on glass; active photocatalysts, Polyhedron 22 (2003) 35–44, doi:http://dx.doi.org/10.1016/S0277-5387(02)01333-5.
[19] B.E. Yoldas, Hydrolysis of titanium alkoxide and effects of hydrolytic polycondensation parameters, J. Mater. Sci. 21 (1986) 1087–1092, doi:http://dx.doi.org/10.1007/BF01117399.
[20] A. Leaustic, F. Babonneau, J. Livage, Structural investigation of the hydrolysis-condensation process of titanium alkoxides $Ti(OR)_4$ (OR = OPr-iso, OEt) modified by acetylacetone. 2. From the modified precursor to the colloids, Chem Mater. 1 (1989) 248–252, doi:http://dx.doi.org/10.1021/cm00002a016.
[21] G. Yi, M. Sayer, Sol-gel processing of complex oxide films, Am. Ceram. Soc. Bull. 70 (1991) 1173–1179.
[22] A. Mills, A. Lepre, N. Elliott, S. Bhopal, I.P. Parkin, S.A. O'Neill, Characterization of the photocatalyst Pilkington Activ™: a reference film photocatalyst? J. Photochem. Photobiol. A160 (2003) 213–224.
[23] A. Mills, J. Wang, Simultaneous monitoring of the destruction of stearic acid and generation of carbon dioxide by self-cleaning semiconductor photocatalytic films, J. Photochem. Photobiol. A182 (2006) 181–186.
[24] A. Mills, N. Elliott, I.P. Parkin, S.A. O'Neill, R.J. Clark, Novel TiO_2 CVD films for semiconductor photocatalysis, J. Photochem. Photobiol. A151 (2002) 171–179.
[25] G. Kenanakis, D. Vernardou, E. Koudoumas, N. Katsarakis, Growth of *c*-axis oriented ZnO nanowires from aqueous solution: the decisive role of a seed layer for controlling the wires' diameter, J. Crys. Growth 311 (2009) 4799–4804, doi:http://dx.doi.org/10.1016/j.jcrysgro.2009.09.026.
[26] G. Kenanakis, D. Vernardou, N. Katsarakis, Light-induced self-cleaning properties of ZnO nanowires grown at low temperatures, Appl. Catal. Part A 411 (2012) 7–14.
[27] D. Vernardou, G. Kalogerakis, E. Stratakis, G. Kenanakis, E. Koudoumas, N. Katsarakis, Photoinduced hydrophilic and photocatalytic response of hydrothermally grown TiO_2 nanostructured thin films, Solid State Sci. 11 (2009) 1499–1502, doi:http://dx.doi.org/10.1016/j.solidstatesciences.2009.05.014.
[28] D. Vernardou, E. Stratakis, G. Kenanakis, H.M. Yates, S. Couris, M.E. Pemble, E. Koudoumas, N. Katsarakis, One pot direct hydrothermal growth of photoactive TiO_2 films on glass, J. Photochem. Photobiol. A: Chemistry 202 (2009) 81–85, doi:http://dx.doi.org/10.1016/j.jphotochem.2008.11.015.
[29] T.Y. Zhang, T. Oyama, A. Aoshima, H. Hidaka, J.C. Zhao, N. Serpone, Photooxidative *N*-demethylation of methylene blue in aqueous TiO_2 dispersions under UV irradiation, J. Photochem. Photobiol. A: Chem. 140 (2001) 163–169, doi:http://dx.doi.org/10.1016/S1010-6030(01)00398-7.
[30] C.H. Kwon, H. Shin, J.H. Kim, W.S. Choi, K.H. Yoon, Degradation of methylene blue via photocatalysis of titanium dioxide, Mater. Chem. Phys. 86 (2004) 78–82, doi:http://dx.doi.org/10.1016/j.matchemphys.2004.02.024.
[31] A. Houas, H. Lachheb, M. Ksibi, E. Elaloui, C. Guillard, J.M. Herrmann, Photocatalytic degradation pathway of methylene blue in water, Appl. Catal. B: Environ. 31 (2001) 145–157, doi:http://dx.doi.org/10.1016/S0926-3373(00)00276-9.
[32] L. Rizzo, J. Koch, V. Belgiorno, M.A. Anderson, Removal of methylene blue in a photocatalytic reactor using polymethylmethacrylate supported TiO_2 nanofilm, Desalination 211 (2007) 1–9, doi:http://dx.doi.org/10.1016/j.desal.2006.02.081.
[33] Y. Paz, Z. Luo, L. Rabenberg, A. Heller, Photooxidative self-cleaning transparent titanium dioxide films on glass, J. Mater. Res. 10 (1995) 2842–2848, doi:http://dx.doi.org/10.1557/JMR.1995.2842.
[34] Y. Lei, L.D. Zhang, J.C. Fan, Fabrication, characterization and Raman study of TiO_2 nanowire arrays prepared by anodic oxidative hydrolysis of $TiCl_3$, Chem. Phys. Lett. 338 (2001) 231–236, doi:http://dx.doi.org/10.1016/S0009-2614(01)00263-9.
[35] B.H. Kim, J.-H. Ahn, J.-H. Jeong, Y.-S. Jeon, K.-O. Jeon, K.-S. Hwang, Preparation of TiO_2 thin film on SiO_2 glass by a spin coating–pyrolysis process, Ceram. Int. 32 (2006) 223–225, doi:http://dx.doi.org/10.1016/j.ceramint.2005.01.016.

[36] T. Giannakopoulou, N. Todorova, T. Vaimakis, S. Ladas, C. Trapalis, Study of fluorine-doped TiO_2 sol–gel thin coatings, J. Sol. Energy Eng. 130 (2008) 5, doi:http://dx.doi.org/10.1115/1.2969804.
[37] T. Wang, H. Wang, P. Xu, X. Zhao, Y. Liu, S. Chao, The effect of properties of semiconductor oxide thin films on photocatalytic decomposition of dyeing waste water, Thin Solid Films 334 (1998) 103–108, doi:http://dx.doi.org/10.1016/S0040-6090(98)01125-0.
[38] K. Sunada, Y. Kikuchi, K. Hashimoto, A. Fujishima, Bactericidal and detoxification effects of TiO_2 thin film Photocatalysts, Environ. Sci. Technol. 32 (1998) 726–728, doi:http://dx.doi.org/10.1021/es970860o.
[39] A. Sadeghzadeh Attar, M. Sasani Ghamsari, F. Hajiesmaeilbaigi, Sh. Mirdamadi, K. Katagiri, K. Koumoto, Synthesis and characterization of anatase and rutile TiO_2 nanorods by template-assisted method, J. Mater. Sci. 43 (2008) 5924–5929, doi:http://dx.doi.org/10.1007/s10853-008-2872-y.
[40] S. Bakardjieva, J. Šubrt, V. Štengl, M.J. Dianez, M.J. Sayagues, Photoactivity of anatase–rutile TiO_2 nanocrystalline mixtures obtained by heat treatment of homogeneously precipitated anatase, Appl. Catal. B: Environ. 58 (2005) 193–202, doi:http://dx.doi.org/10.1016/j.apcatb.2004.06.019.